ICMFF11
International Conference on Multiaxial Fatigue & Fracture
Seville, June 1st-3rd, 2016

Implementation of Fatigue Model for Unidirectional laminate based on Finite Element Analysis: Theory and Practice

D. Carrella-Payan[1], B. Magneville[1], M.Hack[1], T.Naito[2], Y.Urushiyama[2], T.Yokozeki[3], W.Yamazaki[3], W.Van Paepegem[4]

[1] Siemens PLM Software, Leuven (Be), Delphine.carrella@siemens.com
[2] Honda R&D Co Ltd, Tochigi
[3] Department of Aeronautics and Astronautics, The University of Tokyo
[4] Department of Materials Science and engineering, Ghent University

ABSTRACT.
The aim of this study is to deal with the simulation of intra-laminar fatigue damage in unidirectional composite under multi-axial and variable amplitude loadings. The variable amplitude and multi-axial loading is accounted for by using the damage hysteresis operator based on Brokate method [6]. The proposed damage model for fatigue is based on stiffness degradation laws from Van Paepegem combined with the 'damage' cycle jump approach extended to deal with unidirectional carbon fibres. The parameter identification method is here presented and parameter sensitivities are discussed. The initial static damage of the material is accounted for by using the Ladevèze damage model and the permanent shear strain accumulation based on Van Paepegem's formulation. This approach is implemented into commercial software (Siemens PLM). The validation case is run on a bending test coupon (with arbitrary stacking sequence and load level) in order to minimise the risk of inter-laminar damages. This intra-laminar fatigue damage model combined efficient methods with a low number of tests to identify the parameters of the stiffness degradation law, this overall procedure for fatigue life prediction is demonstrated to be cost efficient at industrial level. This work concludes on the next challenges to be addressed (validation tests, multiple-loadings validation, failure criteria, inter-laminar damages…)

INTRODUCTION

The increase of lightweight material in transportation industries is today facing more than ever questions on fatigue life prediction of composite structures. The critical step towards accurate prediction is to reproduce the loading conditions undergone by the composite component. In automotive application, the challenge is related to the variability of those conditions: multi-axial and variable amplitude on long duration fatigue loading. This is why Siemens PLM software has developed an innovative composite fatigue CAE methodology (patent pending) keeping track of the material degradation under such conditions.

Sevenois [1] reviewed and compared the state of the art for fatigue model techniques of woven and UD composite. The study concluded that out of the four modelling methodologies (fatigue life, residual strength, residual stiffness and mechanistic model) the residual stiffness models are suitable for mechanical performance using experimental data and can also be combined with residual strength approach.

The presented methodology is based on residual stiffness fatigue law combined with an efficient damage operator approach to calculate the residual stiffness. This approach will be able to perform fatigue simulations for variable amplitude loads and will allow ply-stacking optimization without additional testing or material characterizations.

INTRA-LAMINAR FATIGUE SOLUTION WITH DAMAGE JUMP

The intralaminar fatigue model strategy is herein presented in the following order: definition of the stiffness degradation law, then calculation optimisation algorithm (N-Jump and damage jump combined to the damage operator) and finally, description of parameter identification procedure used in Siemens PLM commercial software.

Fatigue and Stiffness Degradation – Theory

Fatigue damage laws

The damage evolution law is based on the work of Van Paepegem for woven glass fibers [2]. Three intra-laminar damage variables D_{11}, D_{22} and D_{12} are defined at ply level and linked to the stress tensor by the following behavior law, Eq.(1)

$$\underline{\sigma} = HCH(\underline{\varepsilon} - \underline{\varepsilon}^p) \tag{1}$$

where C is the Stiffness tensor, $\underline{\varepsilon}^p$ is a permanent strain tensor and H is defined as

$$\mathrm{H} = \begin{bmatrix} \sqrt{1-D_{11}} & 0 & 0 & 0 & 0 & 0 \\ 0 & \sqrt{1-D_{22}} & 0 & 0 & 0 & 0 \\ 0 & 0 & 1 & 0 & 0 & 0 \\ 0 & 0 & 0 & \sqrt{1-D_{12}} & 0 & 0 \\ 0 & 0 & 0 & 0 & 1 & 0 \\ 0 & 0 & 0 & 0 & 0 & 1 \end{bmatrix} \tag{2}$$

In [2] the damage variables D_{ij} were split into a positive and a negative part (d_{ij}^+ and d_{ij}^-), where the positive part increases when the stress is positive, and the negative one when it is negative. At the end the two parts were added, including a crack closure coefficient for combination of tension of compression. In this work, only positive stress ratios are used, which means that there is no switch between tension and compression over a cycle and simplifies the problem. Either the stress is always positive and the damage D_{ij} is equal to d_{ij}^+; or it is always negative and it is equal to d_{ij}^-, Eq.(3) .

Besides, the formulations of Van Paepegem [2] must be adapted to unidirectional plies. First of all, to account for the high in-plane orthotropy of unidirectional plies, independent c_i parameters are defined for the three components of the damage.

Therefore, fifteen parameters are used ($C_{i,jk}$) instead of five. For the same reason, the coupling between D_{11} and D_{12} which was implemented for woven is removed for UD: in woven fabrics, matrix de-cohesion clearly affects the stiffness in longitudinal and transverse directions, whereas in unidirectional plies, the effect of matrix degradation on longitudinal behavior can be neglected. However, the coupling between D_{22} and D_{12} remains mandatory and has been maintained. Finally, the deletion of this coupling imposes the addition of a propagation term in the formulation of D_{12}, so that a pure shear load in a ply remains able to lead to its collapse. With these assumptions applied to the formulations taken from [2], the evolution laws for the damage variables become:

$$
\begin{aligned}
\frac{d(d_{11}^{+})}{dN} &= c_{1,11}\Sigma_{11}^{+} exp\left(-c_{2,11}\frac{d_{11}^{+}}{\sqrt{\Delta\Sigma_{11}^{+}}}\right) + c_{3,11}\, d_{11}^{+}{\Sigma_{11}^{+}}^{2} exp\left(c_{5,11}\langle\Sigma_{11}^{+} - c_{4,11}\rangle\right)\\
\frac{d(d_{11}^{-})}{dN} &= \left[c_{1,11}\Delta\Sigma_{11}^{-} exp\left(-c_{2,11}\frac{d_{11}^{-}}{\sqrt{\Delta\Sigma_{11}^{-}}}\right)\right]^{3} + c_{3,11}\, d_{11}^{-}{\Sigma_{11}^{-}}^{2} exp\left(\frac{c_{5,11}}{3}\langle\Sigma_{11}^{-} - c_{4,11}\rangle\right)\\
\frac{d(d_{22}^{+})}{dN} &= c_{1,22}\left(1 + {D_{12}^{f}}^{2}\right)\Sigma_{22}^{+} exp\left(-c_{2,22}\frac{d_{22}^{+}}{\left(1 + {D_{12}^{f}}^{2}\right)\sqrt{\Sigma_{22}^{+}}}\right)\\
&\quad + c_{3,22}\, d_{22}^{+}{\Sigma_{22}^{+}}^{2} exp\left(c_{5,22}\langle\Delta\Sigma_{22}^{+} - c_{4,22}\rangle\right)\\
\frac{d(d_{22}^{-})}{dN} &= \left[c_{1,22}\left(1 + {D_{12}^{f}}^{2}\right)\Sigma_{22}^{-} exp\left(-c_{2,22}\frac{d_{22}^{-}}{\left(1 + {D_{12}^{f}}^{2}\right)\sqrt{\Sigma_{22}^{-}}}\right)\right]^{3}\\
&\quad + c_{3,22}\, d_{22}^{-}{\Sigma_{22}^{-}}^{2} exp\left(\frac{c_{5,22}}{3}\langle\Delta\Sigma_{22}^{-} - c_{4,22}\rangle\right)\\
\frac{d(d_{12}^{+})}{dN} &= c_{1,12}\left(1 + {d_{12}^{-}}^{2}\right)\Sigma_{12}^{+} exp\left(-c_{2,12}\frac{d_{12}^{+}}{2\left(1 + {d_{12}^{-}}^{2}\right)\sqrt{\Sigma_{12}^{+}}}\right)\\
&\quad + c_{3,12}\, d_{12}^{-}{\Sigma_{12}^{-}}^{2} exp\left(c_{5,12}\langle\Sigma_{12}^{-} - c_{4,12}\rangle\right)\\
\frac{d(d_{12}^{-})}{dN} &= c_{1,12}\left(1 + {d_{12}^{+}}^{2}\right)\Sigma_{12}^{-} exp\left(-c_{2,12}\frac{d_{12}^{-}}{2\left(1 + {d_{12}^{+}}^{2}\right)\sqrt{\Sigma_{12}^{-}}}\right)\\
&\quad + c_{3,12}\, d_{12}^{+}{\Sigma_{12}^{+}}^{2} exp\left(c_{5,12}\langle\Sigma_{12}^{+} - c_{4,12}\rangle\right)
\end{aligned}
\tag{3}
$$

where $c_{i,jk}$ are the 15 fatigue material coefficients that must be identified, the fatigue failure indices Σ_{ij} are the ratio between the effective stress and the ultimate strength of the material in the ij component, and

$$
\begin{gathered}
\Sigma_{ij}^{+} = max_{cycle}\left(\Sigma_{ij}\frac{\langle\sigma_{ij}\rangle}{|\sigma_{ij}|}\right);\ \Sigma_{ij}^{-} = max_{cycle}\left(\Sigma_{ij}\frac{\langle-\sigma_{ij}\rangle}{|\sigma_{ij}|}\right)\\
where\ \langle\sigma_{ij}\rangle = \begin{cases} 0, & \sigma_{ij} < 0\\ \sigma_{ij}, & \sigma_{ij} \geq 0 \end{cases}
\end{gathered}
\tag{4}
$$

Accumulated permanent strain

In addition to these damage evolution laws, the model takes into account the permanent strain which appears in the ply due to a cyclic shear loading. Some matrix debris formed by the shear stress is accumulated in the opening matrix cracks during tension stress [2], which leads to a non-reversible deformation of the ply.

The c_9 parameter drives the fatigue permanent strain accumulation following the formulation:

$$\frac{d\gamma_{12}^{p}}{dN} = c_9 max_t\langle\gamma_{12}\rangle\frac{dd_{12}^{+}}{dN} + c_9 max_t\langle-\gamma_{12}\rangle\frac{dd_{12}^{-}}{dN} \quad (5)$$

Initial degradation of the ply

It is also important to consider the effect of the first static loading of the ply on its fatigue damage and strain behavior, as it is not included in the fatigue degradation. Therefore, the static damage and permanent strain are evaluated with a static damage model [2] by running a first non-linear analysis up to the peak load of the cyclic fatigue analysis. The resulting initial damage and permanent strain are imposed as initial state of the fatigue analysis and the first cycle can be computed with a correct stress distribution. The fatigue damage tensor D^f is then added to the initial damage tensor D^s

$$D = D^s + D^f \quad (6)$$

The same operation is done with the permanent strain.

Calculation optimisation: from N-Jump to Damage Jump

Block loading: N-Jump

The purpose of the N-Jump algorithm is to avoid running a full FE analysis at each load cycle and to deliberately choose a few relevant load cycles only. The cycles with no significant damage growth are "jumped".

From a first FE analysis, at each Gauss point of the FE model, the theoretical number of cycles to jump NJUMP1 is estimated by extrapolating the damage, Eq. (1) and applying to Eq. (7)

$$\Delta D = D_{N+NJUMP1} - D_N = \begin{cases} 10^{-20}\ if\ D = 0 \\ 0.5D\ if\ 0 < D \leq 0.2 \\ 0.1\ if\ D > 0.2 \end{cases} \quad (7)$$

A global cycle jump NJUMP is defined such that P% of Gauss points verify NJUMP1 < NJUMP for the three components. The value of P has been set to 5% in this study. The damage is finally extrapolated after NJUMP, using again the progressive damage formulations Eq.(3). To validate this algorithm and the value of P, three similar fatigue analyses (three points bending) have been run on the first 100 loading cycles with a 45 degrees layup; one without NJUMP, one with P=1% and one with P=5%. Figure 1 compares the stiffness degradation observed in the three analyses and validates the accuracy of the NJUMP algorithm.

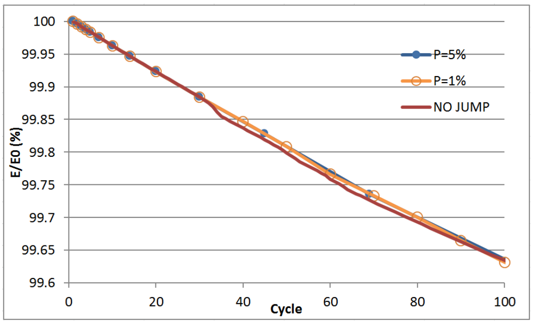

Figure 1: Effect of the N-Jump algorithm on stiffness degradation

Variable Amplitude: Damage Accumulation Jump and Damage hysteresis operator

In automotive industry, the synthesis of realistic fatigue loading involves complex load schedules for different roads with variable loading (Figure 2). The aforementioned jump algorithm is given for block loading. Also, the N-Jump is calculating the damage status by extrapolation (Eq. 7). Here, the damage accumulation jump aims to accurately calculate locally the progressive damage and stiffness degradation.

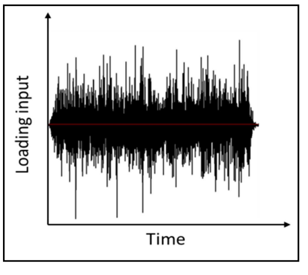

Figure 2. Variable Amplitude example in automotive application

For variable amplitude, traditional fatigue approaches for metallic material use SN curves, linear Miner-Palmgren damage accumulation and cycle (rainflow) based damage evaluations [3-5]. SN curves are test based on curve fitting techniques which does not take into account the loading history of the material. In 1945, Miner developed a linear damage accumulation method, based on the work of Palmgren and added the contribution of various stress amplitude loading to the damage. However, as for SN curves, the loading history of the material is not accounted for. In Rainflow counting methods the damage level depends on full closing hysteresis loops of load cycles (Figure 3).

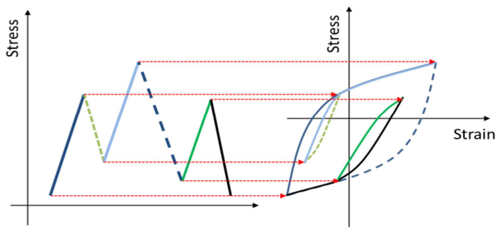

Figure 3. Illustration of rainflow method based on stresses/strains with nested cycles

In the case of composite materials, the fatigue behavior is changing over time due to changes in the matrix damage state. When applying variable amplitude loading, the largest load cycles – that contribute to the larger amount of damage – commonly take a very long time to complete, due to the many nested cycles (Figure 3). In this case the approach to only consider cycles when they are completed can no longer be justified.

The damage hysteresis operator approach based on Brokate works [6] is able to calculate damage at defined time increment instead of 'closed load increment'. This operator allows to up-date the damage status depending on the pre-damage and any other external factors (i.e. temperature, humidity…). These operators are therefore suited to follow the progressive damage curves and also to include damage history of the material. This approach gives good prediction when applied to temperature dependent fatigue analysis with non-linear damage accumulation [7-8-9] and for full car structures with full load histories [10].

PARAMETER IDENTIFICATION PROCEDURE

Tests protocol

In this study, two different tests protocols are proposed. The first one is a traditional approach with tensile tests on five layups and five load levels per layup capturing a representative span of fatigue life (based on test method [11]). This results in twenty five configurations. The second one is a trial of a more innovative approach with one-sided bending tests on the same five layups, but with only one load level for each layup, so only five configurations. The idea is to assess if the load distribution on this kind of specimen can provide enough information to feed the damage model, as a three-points-bending test results in progressive load levels along the same specimen, both in tension and compression.

Comment [MHA1]: an application

Peak data such as load, displacement, strains from extensometers and gauges, temperature are measured from these tests at several representative cycles. The stiffness degradation of each specimen can be estimated from these evolutions. Additionally, running-in and unloading raw data are extracted to analyse the initial stiffness drop of the specimens and their final permanent strain.

Parameters identification protocol

The parameters identification consists in an FE-based optimization of the fifteen fatigue parameters to fit simulated stiffness degradation with experimental results. A step-by-step methodology identifying the parameters one by one from specific experimental data has been setup. As illustrated by two examples in [Figure 4], each c_i parameter has a specific contribution on the numerical stiffness degradation, and therefore can be adjusted to perfectly fit with experimental results.

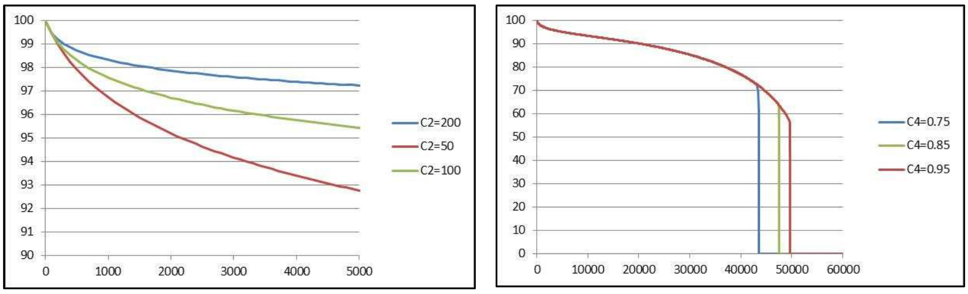

Figure 4: Effect of $c_{2,12}$ (left) and $c_{4,12}$ (right) on numerical stiffness degradation

Therefore, two volume finite elements models reproducing the two testing procedures have been created, and the nonlinear fatigue solver with N-Jump algorithm is used to efficiently correlate the stiffness degradation of each testing configuration by adjusting the fifteen $c_{i,jk}$ parameters (note that the N-Jump is herein used as tests are carried out under constant amplitude loading). An illustration of the resulting correlation between experimental and simulated stiffness evolutions is given in [Figure 5].

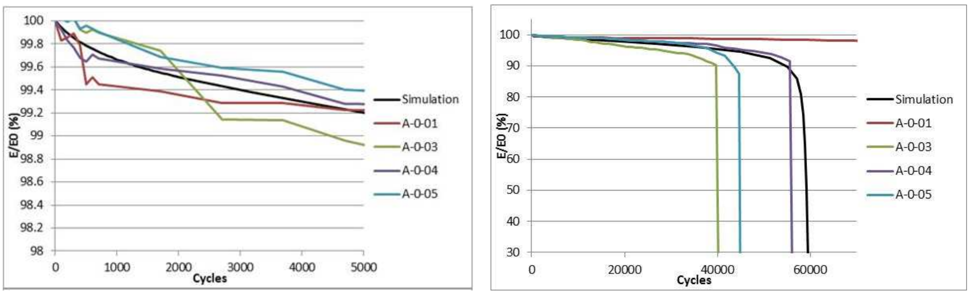

Figure 5: Correlation between experimental and simulated stiffness evolutions ($[0]_{20}$ layup in 3Pts Bending)

Finally, the parameter c_9 is estimated by crosschecking the raw data of the unloading of some of the specimens.

VALIDATION/APPLICATION

The first validation has been conducted on a coupon at constant amplitude loading. The same three points bending analysis as above is run on 80 000 cycles at an imposed load level. A more complex quasi-isotropic layup $[0/60/-60]_{4s}$ is now studied. The resulting stiffness degradation is compared to experimental data [Figure 6]. The good predictability illustrates the main interest of a ply-level damage law: identification is performed on specific layups, and the resulting material data remains available for any layup without additional identification.

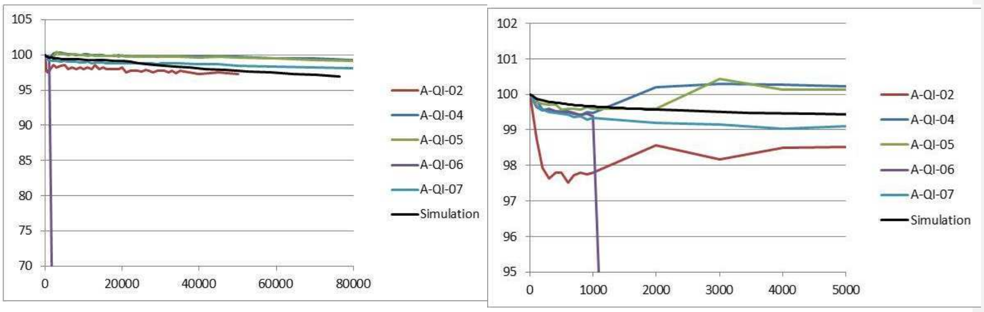

Figure 6: Predictability of stiffness reduction of a 3Pts-bending quasi-isotropic coupon

Further validation cases have been investigated (i.e. flat and V-shaped components) but the overall stiffness degradation contribution from the fatigue loading in these cases were due to the interlaminar delamination. Additional validation cases are under investigations to account for higher stiffness degradations.

This brings to the next challenges to extend this methodology to a complete intralaminar and interlaminar fatigue damage solution for variable amplitude and multi-axial loadings.

REFERENCES

1. **Sevenois, R.D.B., Van Paepegem, W.** (2015). *Appl. Mech. Reviews*, **67**
2. **Van Paepegem W.** (2002). PhD Thesis, Ghent University, Belgium.
3. **Miner, M.A**, (1945) *Journal of Applied Mechanics*, **67**, A159-A164
4. **Matsuishi, M.; Endo, T.,** (1968) *Japanese Society of Mech. Eng.*, Fukuoka, Japan
5. **Dowling, N. E.**, (1972) *Journal of Materials, JMLSA*, **7**(1), 71-87
6. **Brokate, M; Dressler, K; Krejci, P.,** (1996), *Eur. J. Mech. A/Solids*, **15**, 705-737
7. **Nagode, M., Hack, M.,** (2011) *SAE Int. J. of Mat. & Manuf.*, **4** (1), 632-637
8. **Nagode, M., Hack, M., Fajida, M.**, (2010) *Fat. Fract Mat. Struct.* **33**(3), 149-160
9. **Šeruga, D., Hack, M., Nagode, M.** (2016), *MTZ worldwide*, **77**(3),44-49
10. **Brune, M., et al.**, (1998) *Fatigue Design'98*, Helsinki
11. **ASTM D3479**, (2015) *Sapce Simulation, composite mat.*, **15.03**